1

Nuclei in the Cosmos

> There is a coherent plan in the universe, though I don't know what it's a plan for.
>
> *Fred Hoyle*

In order to understand about the composition of stars and how they produce energy, we need to know about nuclei, and about the reactions which they undergo. This chapter provides an introduction to the description of nuclei, and surveys the range of scenarios in which important reactions occur. We begin with the Big Bang, then discuss energy production cycles in stars, and finish with an outline of some of the processes by which we think that heavy elements are produced in supernovae and other stellar enviroments. The more detailed discussion of nuclear physics begins in Chapter 2, to which the more advanced student is directed.

1.1 Nuclei

1.1.1 Properties of nuclei

Each isotope (A, Z), characterized by *mass number* A and charge Z, has in its ground state a rest mass $m_{A,Z}$. This total mass is less than the sum of the masses of the constituent protons and neutrons due to the binding energy of the system. Energy is released when the bound state is formed. The binding energy may be calculated by

$$B(A, Z) = (Zm_p + Nm_n - m_{A,Z})c^2, \tag{1.1.1}$$

and is the energy required to break up the nucleus into its A constituent nucleons. The number of neutrons is $N = A - Z$. A unit atomic mass is (1 u) has rest energy $mc^2 = 931.494\,\text{MeV}$.

The *binding energy per nucleon* B/A dictates whether energy must be supplied or will be released in the fusion of two nuclei to form their composite. The values of $B(A, Z)/A$ are shown in Fig. 1.1 for all the long-lived isotopes. The larger the energy one needs to supply to release a nucleon, the more stable is the nucleus. The most

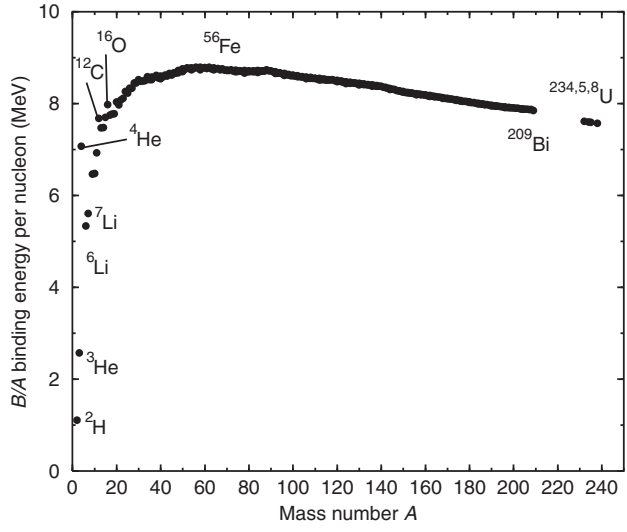

Fig. 1.1. Binding energies per nucleon, $B(A,Z)/A$, for all naturally occurring long-lived isotopes of A nucleons.

stable isotopes are near ^{56}Fe, as seen from Fig. 1.1. If two nuclei A_1 and A_2 fuse to form $A = A_1 + A_2$, then the reaction is typically exothermic and energy is released if $A \lesssim 56$. If $A \gtrsim 56$ then fusion reactions are typically endothermic – energy is required – so we might expect the opposite process, *fission*, to be more likely. Fission occurs spontaneously for many nuclei $Z \gtrsim 90$, called the *actinides*.

The most stable nuclear isotopes for $Z \lesssim 20$ have $N \approx Z$, whereas heavier nuclei tend to have more neutrons, to compensate for the increased Coulomb repulsion. If we make a plot with N as the horizontal axis and Z as the vertical axis, we have the Segré chart of Fig. 1.2. Each row is a distinct chemical element, and the stable isotopes are the dark squares lying roughly along the diagonal. The naturally-occurring nuclei, with the longest lifetimes, are said to occupy the *valley of stability*. Neutron-rich nuclei are shown below, to the right of the valley of stability, out to the *neutron dripline*, the point beyond which one cannot form bound states, no matter how many neutrons are added to the system. There is a large gulf between observed isotopes and the predicted neutron dripline, especially for heavy elements.

Conversely, proton-rich nuclei, although they are not so numerous, can be seen above the central valley out to the dripline where proton emission (proton radioactivity) occurs. Most proton-rich nuclei for $A < 200$ have been observed. Nuclei between the driplines have ground states that are stable to nucleon emission, but may still slowly β-decay (see Section 2.2 for timescales) by the weak interaction (see for example the reactions 1.2.4), or radioactively decay (also slowly) by fission or α-particle emission.

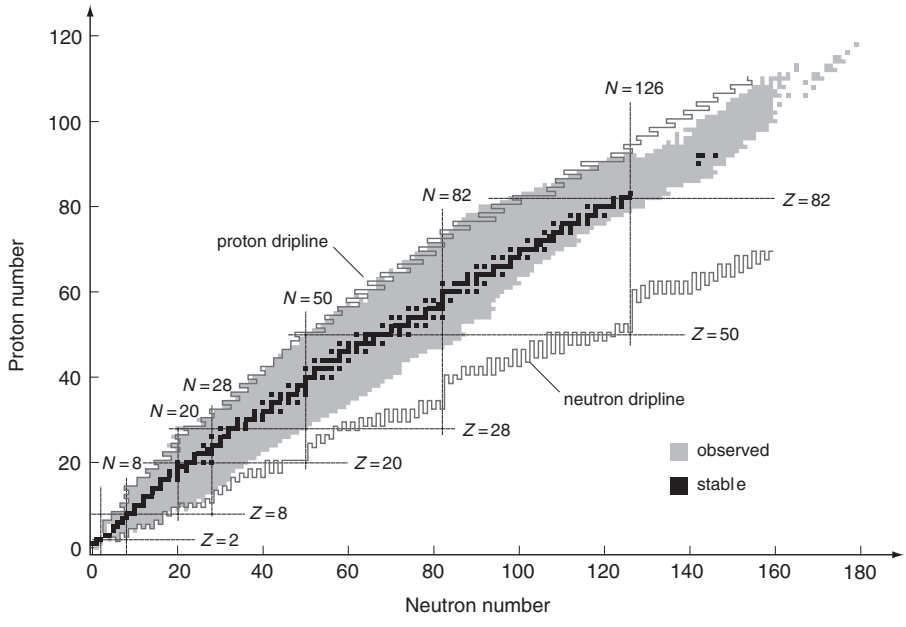

Fig. 1.2. Chart of stable and radioactive isotopes. Vertical and horizontal lines represent magic numbers. Figure courtesy of Marc Hausmann.

1.1.2 Nuclear reactions

If a nuclear reaction is performed in a laboratory, let the *projectile* be called A, the *target* called B, and the *residual nuclei* be C and D. The combination of A and B is called the *entrance channel*, and that of C and D is called an *exit channel* (more than one final channel may be possible). Then the reaction is labeled B(A,C)D, which is the common way of writing

$$\mathrm{A} + \mathrm{B} \rightarrow \mathrm{C} + \mathrm{D}. \tag{1.1.2}$$

Given all the isotopic mass values, we may calculate the energy required or released. This energy, called the Q-value for the reaction, is

$$Q = (m_{\mathrm{A}} + m_{\mathrm{B}} - m_{\mathrm{C}} - m_{\mathrm{D}})c^2. \tag{1.1.3}$$

Exothermic reactions have $Q > 0$, whereas a $Q < 0$ reaction is endothermic.

1.1.3 Forces in nuclei

There are four forces in nature: the *strong*, *electromagnetic*, *weak* and *gravitational* forces. The strong or *nuclear* forces are dominant in binding nuclei, but the other

forces still have important roles to play in nuclear astrophysics. The *electromagnetic* force is responsible for the Coulomb repulsion between protons in nuclei, and the decrease in binding for heavy nuclei seen in Fig. 1.1. The *weak* interaction plays a role whenever reactions involve neutrinos; we will see some examples of this later in this chapter (Eqs. (1.2.1) and (1.2.4)). The *gravitational* attraction is not significant inside nuclei, but is responsible for creating galaxies and stars in the first place, and then compressing them to the stage where nuclear reactions begin.

1.1.4 The Coulomb barrier

In order that a nuclear reaction takes place, the nuclei involved have to be close to each other, but this is hindered by the Coulomb repulsion between the protons, which acts at longer distances compared with the nuclear force of short range. The overall potential energy between two charged nuclei separated by a distance R therefore follows the pattern shown in Fig. 1.3. There is a repulsive *Coulomb barrier* of height V_B, and scattering at energies $E < V_B$ still exists because of quantum tunneling through the barrier.

The exponential reduction of reaction rates for charged particles reacting at low relative energies will be extremely important in all astrophysical scenarios,

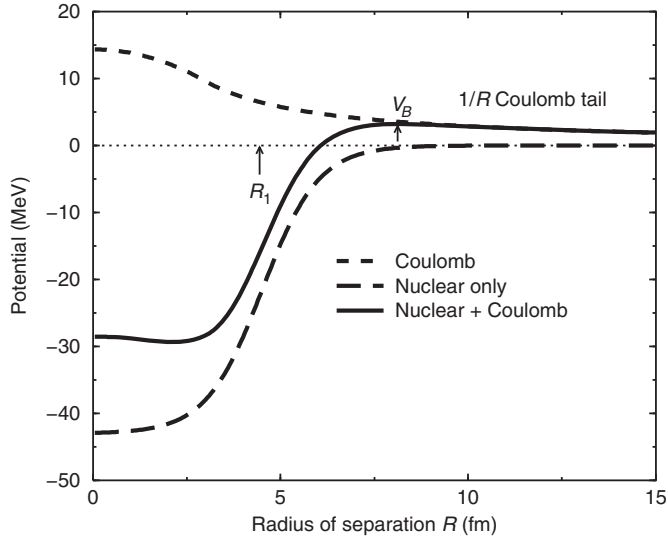

Fig. 1.3. The nuclear and Coulomb potential energies between a proton and ^{40}Ca as a function of the distance R between their centers, where R_1 is the radius of ^{40}Ca. The combined potential (solid line) has a maximum height of V_B, forming the Coulomb barrier.

and will very often be the limiting factor for nuclear reactions. We will see (Section 2.4) that reaction rates are defined by the quantity σ, called the *cross section*. Because cross sections $\sigma(E)$ drop rapidly with decreasing center-of-mass energy E, due to the Coulomb repulsion, we factorize out a simple energy dependence according to

$$\sigma(E) = \frac{1}{E} e^{-2\pi\eta} S(E) \tag{1.1.4}$$

to define an *astrophysical S-factor* $S(E)$ which should vary less strongly with energy. The $1/E$ geometrical factor is associated with the wavelength of the incoming particle, and the exponential factor represents the penetrability through the Coulomb barrier. It depends on η, the *Sommerfeld parameter*, defined as $\eta = Z_1 Z_2 e^2/(\hbar v)$ (Eq. (3.1.71)) where $Z_1 Z_2 e^2$ is the product of charges and v the relative incident velocity. In Fig. 1.4 we show, in the upper panel, the cross section for the α capture on ^{3}He to synthesize ^{7}Be. The reaction cross section falls off rapidly as the energy decreases, whereas the S-factor, shown in the lower panel, is nearly constant.

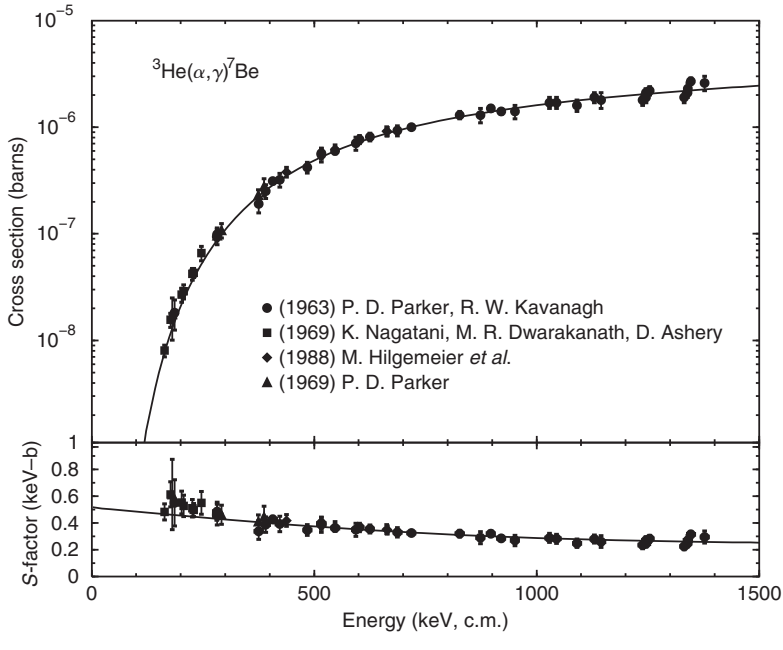

Fig. 1.4. Dependence of cross section and $S(E)$ on energy, for the reaction ^{3}He$(\alpha,\gamma)^7$Be. The solid curve is a calculation to be discussed in Appendix B.

1.2 Primordial nucleosynthesis

Having seen how nuclei and their reactions can be characterized, we now look at a range of nuclear reactions in astrophysics, starting at the beginning. A schematic illustration of the evolution of the Universe immediately after the Big Bang is presented in Fig. 1.5 and briefly described in this section.

Following the Big Bang, the Universe expanded and cooled with a temperature of $T_9 \approx 15/\sqrt{t}$ for time t in seconds and temperature T_9 in units of GK $= 10^9$ K. According to thermodynamics, this temperature corresponds to an energy of $E = k_B T$, where the Boltzmann constant is $k_B = 1.38 \times 10^{-23}$ J K^{-1} $= 0.0861$ MeV GK^{-1}. This means that the material in the expanding Universe had an average thermal energy of $E \approx 1.3/\sqrt{t}$ MeV.

For very early times, $t < 1$ s, the thermal energy E was greater than 1 MeV. In particular, E was greater than $(m_n - m_p)c^2 = 1.24$ MeV, the difference in the rest energies of the neutron and proton. At these times, therefore, there was enough radiative energy available to easily convert neutrons to protons, and back again, in

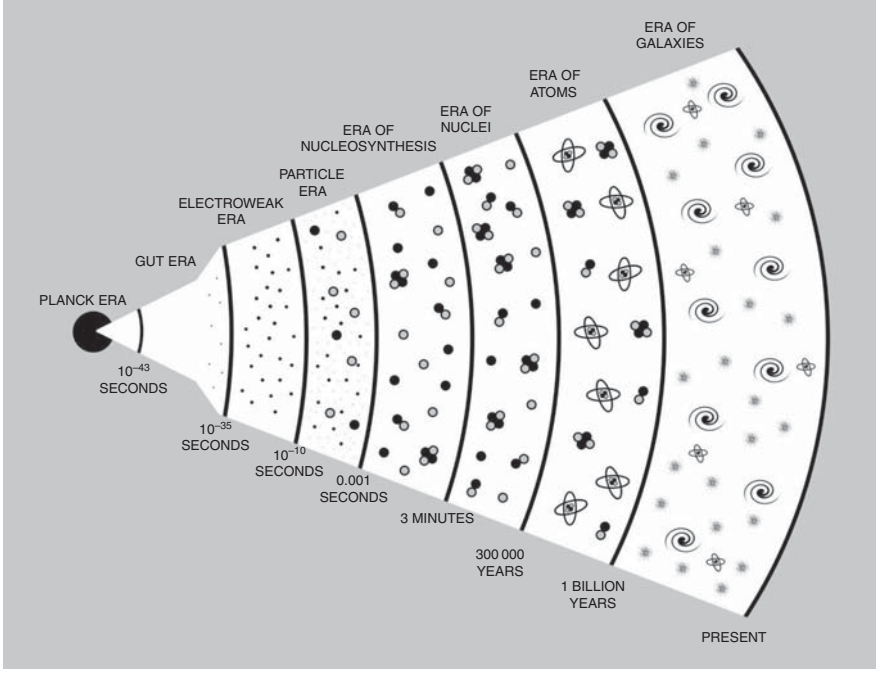

Fig. 1.5. History of the Universe, from the Big Bang to present times. Figure courtesy of Jon Whiting.

a statistical equilibrium by processes such as

$$\begin{aligned} \mathrm{n} + \mathrm{e}^+ &\rightarrow \mathrm{p} + \overline{\nu}_\mathrm{e} \\ \mathrm{p} + \mathrm{e}^- &\rightarrow \mathrm{n} + \nu_\mathrm{e} \\ \mathrm{e}^- + \mathrm{e}^+ &\leftrightarrow \gamma + \gamma \end{aligned} \tag{1.2.1}$$

where γ are photons, and ν_e and $\overline{\nu}_e$ are electron neutrinos and anti-neutrinos. The electrons e^- and positrons e^+ are commonly called *beta* (β) particles. The third reaction of (1.2.1) is the annihilation/production of electron-positron pairs in the high-temperature radiation environment.

Only after two seconds did the Universe cool down enough to enable the neutrons and protons to retain their identities ($E \lesssim 1\,\mathrm{MeV}$); this was the beginning of the astrophysics of nuclei. At this point there begun a period of about 250 s in which a *primordial nucleosynthesis* took place, and neutrons and protons combined to form hydrogen and helium isotopes, and perhaps a few lithium nuclei. At the beginning of this period there were only neutrons and protons, with a relative number density determined by their mass difference according to the Saha equation

$$\frac{n_n}{n_p} \approx \exp\left[-\frac{(m_n - m_p)c^2}{k_B T}\right], \tag{1.2.2}$$

an equation that will be derived in Chapter 12. When $k_B T \gg (m_n - m_p)c^2$, we have $n_n \approx n_p$. As the temperature dropped, there was a *freeze-out* in which the small $m_n - m_p$ difference led to the residual neutron and proton ratio of $n_n/n_p \sim 1/8$. This ratio may be found from a calculation that balances the cooling rate with the actual transition rates of the reactions (1.2.1) above.

Two protons or two neutrons cannot form a bound state, but a neutron and a proton may collide and form a deuteron, abbreviated d or ^{2}H. This reaction releases energy ($Q = 2.226\,\mathrm{MeV}$) in the form of a photon and the recoil energy of the deuteron:

$$\mathrm{n} + \mathrm{p} \rightarrow \mathrm{d} + \gamma. \tag{1.2.3}$$

This is what we call a *capture reaction*. These deuterons react easily with other protons and neutrons, giving rise to a series of reactions, the dominant ones of which are illustrated in Fig. 1.6. Tritons ^{3}H (t) can be formed, the hydrogen isotope with one proton and two neutrons, as well as helium isotopes with two protons and either one neutron (^{3}He) or two neutrons (^{4}He). The binding energy of the deuteron is one of the most fortunate coincidences in the Universe. The Universe took about 7 minutes to cool down to 2.226 MeV, and the neutron lifetime is slightly above

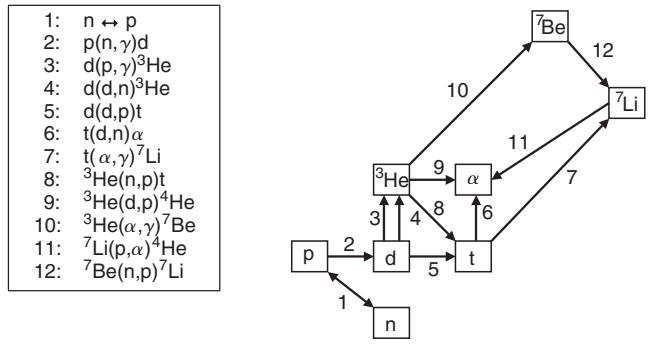

Fig. 1.6. The dominant reactions in primordial nucleosynthesis, after Kawano [1].

7 minutes. Had these two numbers not properly matched, there would have been no neutrons to initiate the whole primordial nucleosynthesis.

By time $t \approx 250$ s, the thermal energy E was 0.1 MeV, and all these primordial reactions came to a stop, except for the decays of neutrons, tritons and ^{7}Be. These last three nuclei were produced in primordial nucleosynthesis, but are not themselves stable, as they decay with lifetimes of 10.3 minutes, 12.3 years and 53 days, respectively, by *weak interactions* in what is called *β-decay*:

$$\begin{aligned} \mathrm{n} &\rightarrow \mathrm{p} + \mathrm{e}^- + \overline{\nu}_\mathrm{e}, \\ \mathrm{t} &\rightarrow {}^3\mathrm{He} + \mathrm{e}^- + \overline{\nu}_\mathrm{e}, \\ {}^7\mathrm{Be} &\rightarrow {}^7\mathrm{Li} + \mathrm{e}^+ + \nu_\mathrm{e}. \end{aligned} \tag{1.2.4}$$

Eventually, all the neutrons and radioactive nuclei transmuted into stable nuclei, such that only very small fractions of ^{7}Li, and practically no ^{6}Li remained. As a consequence, the initial composition of the Universe was almost entirely p, d, ^{3}He, ^{4}He, e^-, γ particles and neutrinos. This primeval ratio of abundances, listed in Table 1.1, can still be observed if we avoid regions where further reactions have taken place, such as in low-metal stars.

Very few nuclei heavier than helium are formed at this stage. One reason for this is that there are no stable nuclei with 5 nucleons, nor with 8 nucleons. The longest-lived isotopes with 5 nucleons are ^{5}He and ^{5}Li, but these emit neutrons and protons respectively. For element production there are thus bottlenecks at mass numbers of 5 and 8 that had to be later bridged by other means.

Very little further happened until the Universe reached time $t = 3.8 \times 10^5$ y, when the temperature and energies were low enough ($T \sim 4 \times 10^3$ K and $E \sim 0.4$ eV) for electrons to remain bound to nuclei in atoms. At that point, the atomic era started. After $t \sim 10^9$ y, stars and galaxies were formed, giving way to stellar

Table 1.1. *Isotopic abundances Y_i from primordial nucleosynthesis [2], defined by the fraction of nuclides i to the number of all nucleons. The nucleon number density is then $X_i = A_i Y_i$ of nucleons in that isotope of mass A_i. Normalization is $\sum_i X_i = 1$.*

Isotope	Nuclide fraction Y_i	Nucleon fraction X_i
^{1}H = p	0.75	0.75
^{2}H = d	2.44×10^{-5}	4.88×10^{-5}
^{3}He	1.0×10^{-5}	3.0×10^{-5}
^{4}He	0.062	0.2481
^{6}Li	1.1×10^{-14}	6.6×10^{-14}
^{7}Li	4.9×10^{-10}	34.3×10^{-14}

nucleosynthesis. Eventually some stars collapsed, heated up, and completely new cycles of nuclear reactions took place. This was how many heavier nuclei were produced. These processes continued to repeat themselves until the present day.

1.3 Reactions in light stars

After stars are formed by gravitational attraction, their continued contraction compresses the constituent gases and raises their temperature. If the star has a mass above a minimum of about 0.1 solar masses ($0.1\,M_\odot$), then the temperature rises to $T \sim 10{-}15 \times 10^6$ K and the density to $\rho \sim 10^2\,\mathrm{g\,cm^{-3}}$, and *nuclear hydrogen burning* can start. The release of energy in the resulting nuclear reactions is sufficient to stop further gravitational collapse, and the star remains in a phase of hydrostatic equilibrium. The compressive gravitational pressure is balanced by the expansive gas pressure of material heated by the nuclear reactions. Different initial stellar masses give rise, in this phase, to the range of main sequence stars represented in Fig. 1.7. The Hertzsprung-Russell diagram (H-R diagram) is a standard representation of stars in terms of their surface temperature and luminosity. Many stars are aligned roughly according to Stefan's law of $L \propto R^2 T^4$, and form what is called the main sequence. This corresponds to stars in their hydrogen-burning phase.

1.3.1 Proton-proton chains

The first series of nuclear reactions in a new star with mass $M < 1.5\,M_\odot$ is the *proton-proton chain*. This has the overall effect of converting 4 protons into one

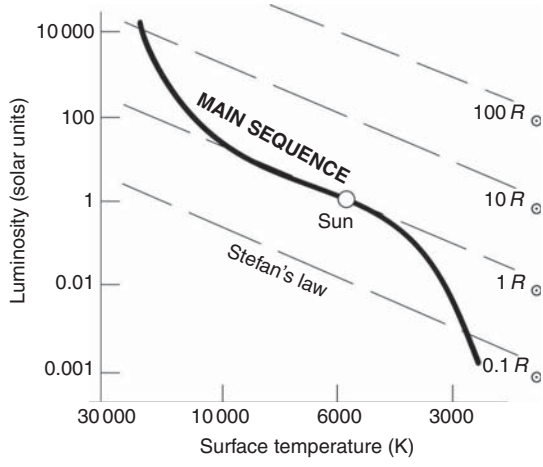

Fig. 1.7. H-R diagram: main sequence stars are represented by the thick curve, whereas the thin lines represent Stefan's law. Figure courtesy of Jon Whiting.

α particle (a ^{4}He nucleus), along with two positrons (2 e^+), two neutrinos (2 ν), and 26 MeV of released energy. It does not do this in one step, but via a chain that starts with

$$p + p \rightarrow d + e^+ + \nu_e \qquad (Q = 1.44\,\text{MeV}). \tag{1.3.1}$$

This reaction, involving neutrinos, proceeds by the *weak interaction*, and has a very low reaction rate. In fact, its rate is so low that it has never been measured directly. The slowness of this initial step is what is responsible for the long lifetime of stars in their hydrogen-burning phase.

Following the formation of the deuteron d (^{2}H), a subsequent proton capture reaction

$$d + p \rightarrow {}^3\text{He} + \gamma \qquad (Q = 5.49\,\text{MeV}) \tag{1.3.2}$$

may readily occur. The reaction $d + d \rightarrow {}^4\text{He} + \gamma$ may also occur, but is less likely since protons are much more abundant than deuterons at this stage: about 1 deuteron for every 10^{18} protons.

A second proton capture on ^{3}He cannot succeed because ^{4}Li is unbound, but other possible reactions involving ^{3}He are (in Chain I):

$${}^3\text{He} + {}^3\text{He} \rightarrow {}^4\text{He} + 2p + \gamma \qquad (Q = 12.86\,\text{MeV}), \tag{1.3.3}$$

or

$${}^3\text{He} + {}^4\text{He} \rightarrow {}^7\text{Be} + \gamma \qquad (Q = 1.59\,\text{MeV}). \tag{1.3.4}$$

The ^{7}Be does not last long, but produces two α particles, using either Chain II

$$^7\mathrm{Be} + \mathrm{e}^- \rightarrow {}^7\mathrm{Li} + \nu_\mathrm{e} \tag{1.3.5}$$

$$^7\mathrm{Li} + \mathrm{p} \rightarrow {}^4\mathrm{He} + {}^4\mathrm{He}, \tag{1.3.6}$$

or Chain III

$$^7\mathrm{Be} + \mathrm{p} \rightarrow {}^8\mathrm{B} + \gamma \tag{1.3.7}$$

$$^8\mathrm{B} \rightarrow {}^8\mathrm{Be} + \mathrm{e}^+ + \nu \tag{1.3.8}$$

$$^8\mathrm{Be} \rightarrow {}^4\mathrm{He} + {}^4\mathrm{He}, \tag{1.3.9}$$

where the ^{8}Be is a narrow resonance at 92 keV with width 6.8 eV. Resonances will be characterized in detail in Chapter 3: they are long-lived combinations of the reacting nuclei that are produced in specific circumstances. This particular ^{8}Be resonance will appear again later in this chapter when we discuss the triple-α process.

Figure 1.8 illustrates the three branches of the pp chain, in which the total energy released is the same (26.73 MeV). However, the energy carried by the neutrinos is lost to the star since neutrinos have a negligible probability for subsequent collisions. The energy retained in the star, Q_ret, is 26.20 MeV for Chain I, 25.66 MeV for Chain II, and 19.17 MeV for Chain III. This is the energy that is responsible for heating the star, and hence also its emission of light. It also, for a long while, prevents any further gravitational collapse.

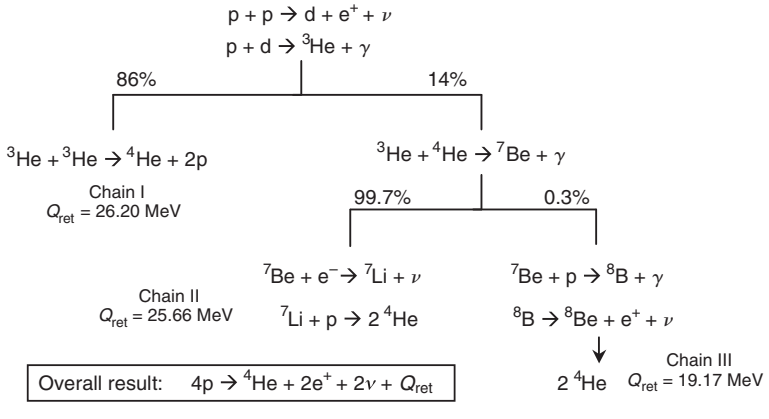

Fig. 1.8. The proton-proton chain has three branches, I, II, and III, which retain different quantities of energy Q_ret within the star.

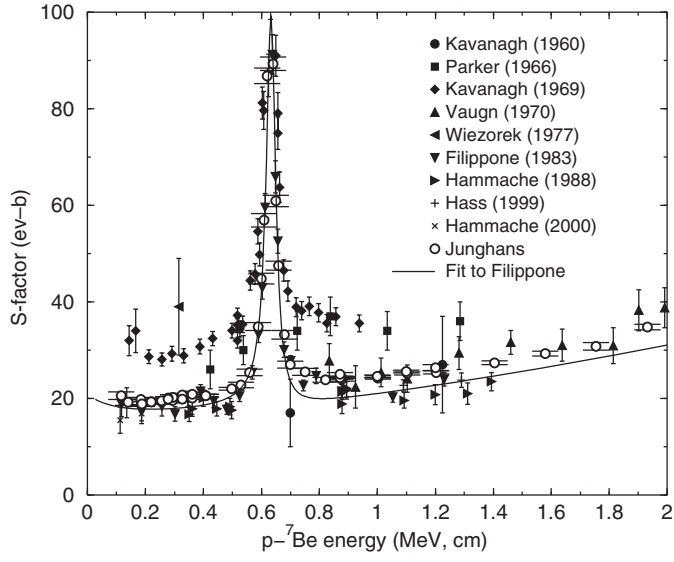

Fig. 1.9. Measured astrophysical S-factors $S(E)$ for the ^{7}Be(p,γ)^{8}B reaction, with the 1^+ resonance at 640 keV. The astrophysical rate is needed at $\approx$ 20 keV, requiring downward extrapolations from the experimental energies. The curve is an E1 direct capture model combined with an M1 resonance in a hybrid R-matrix treatment, fitted to the Filippone data.

Many of these reactions have been measured in the laboratory, all the way down to energies relevant for the stellar environment ($E \approx 0.1$ MeV). An example is shown in Fig. 1.4 for ^{4}He(^{3}He,γ)^{7}Be: cross sections decreasing exponentially at small energies are shown in the upper half and S-factors, nearly constant with energy, are shown in the lower half. As mentioned before, the cross section for fusions of charged particles is strongly dependent on energy because of the Coulomb barrier. Most of the energy dependence is given by the $e^{-2\pi\eta}/E$ factor in Eq. (1.1.4), which will be derived in Chapter 7.

For the ^{7}Be(p,γ)^{8}B reaction, the S-factor is only constant away from the 1^+ resonance at 640 keV that is prominent in Fig. 1.9. Reaction theory will be needed to describe how these resonances are superimposed upon the smoother non-resonant background cross sections. In addition, different data sets shown in Fig. 1.9 have different normalizations at low energies, where the measurement is hardest.

Both reactions, ^{4}He(^{3}He,γ)^{7}Be and ^{7}Be(p,γ)^{8}B, are not important for the energy production of a star. However they are connected to the amount of neutrinos emitted from the star and are very important contributions to the solar neutrino experiments [3].

1.3.2 Triple-α reaction

As mentioned earlier, there are no stable nuclei with $A = 5$ or 8 nucleons. We saw that the Big Bang production of ^{6,7}Li is very low, and so it is difficult to produce nuclei of mass $A \geq 9$ in stars. There are many α particles, but they do not form another binary bound state with themselves, with protons, or with neutrons. Fortunately, the narrow low-lying resonance in $^8\text{Be} = \alpha + \alpha$ does trap them together in pairs with some small probability, and this probability is large enough for a third α particle to collide with the resonance pair to form a *triple-α* composite. This composite is an excited state in ^{12}C, and can either decay back to 3α, or, with a small branching ratio, decay to lower-energy bound states in ^{12}C by γ emission and e^+e^- production.

The non-resonant direct triple-α reaction does not produce enough carbon to explain the observed abundance. The key point is a narrow 0^+ resonance in the $^8\text{Be} + \alpha = {}^{12}\text{C}^*$ system that enhances the triple-α fusion reaction. This is shown in Fig. 1.10. This resonance is called the *Hoyle resonance*, after the person who predicted it in 1954 [4] on the basis that this was the only way to produce the measured quantities of ^{12}C in the Universe. The Hoyle resonance was subsequently found by experiments, at 287 keV above the 3α breakup threshold, with a narrow width of 8.3 eV [5]. The decay of the Hoyle resonance is via γ emission to the 2^+ excited state of ^{12}C at 4.44 MeV, or via direct e^+e^- decay to the 0^+ ground state. We will see in Chapter 3 that γ-decays cannot directly couple two 0^+ states.

The equilibrium population of the $2\alpha = {}^8\text{Be}$ resonance can be determined by a Saha equation, like Eq. (1.2.2), where the numerator in the exponential is now the resonance energy of 92 keV. When the temperature $T_9 = 0.3$ and the density $\rho \sim 10^5$ g/cm^3, as typical for He burning, then the resonance population is $N(^8\text{Be})/N(\alpha) \sim 10^{-10}$. This then enables $^8\text{Be} + \alpha \rightarrow {}^{12}\text{C}$ reactions, each of

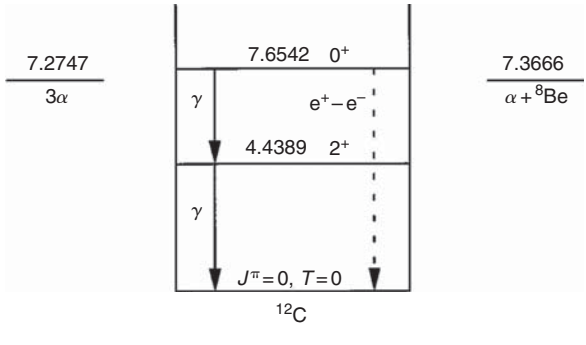

Fig. 1.10. Diagram showing the relevant states in ^{12}C for the triple-α reaction.

which releases an energy $Q = 7.27\,\text{MeV}$. The net result is $3\alpha \rightarrow {}^{12}\text{C}$, the triple-$\alpha$ reaction. Statistical equilibrium will be discussed in detail in Chapter 12.

Strongly connected to the triple-α reaction is the ${}^{12}\text{C}(\alpha,\gamma){}^{16}\text{O}$. The rate of this reaction, relative to the 3α capture, determines the post-He burning C/O ratio, which, in turn, affects the abundances of heavier elements produced in subsequent phases. At present, the C/O ratio is believed to play a crucial role in the last phases of a massive star. In particular, whether the final remnant following a supernova explosion is a neutron star or a black hole is affected by this ratio [6]. Because the 3α reaction is comparatively well known, the ${}^{12}\text{C}(\alpha,\gamma){}^{16}\text{O}$ reaction is still the most important source of uncertainty in the C/O ratio.

1.3.3 CNO cycles

In some stars there will be small fractions of carbon nuclei, either from the 3α reaction or from the remnants of earlier stars that have completed their evolutionary cycle. If these new stars are heavy enough ($M > 1.5\ M_{\odot}$), then the internal temperature is high enough ($T_9 > 0.03$) that there is another cycle that burns hydrogen into helium, but proceeds at a faster rate. This is the CNO cycle illustrated in Fig. 1.11, which uses the initial carbon as a catalyst: it is not consumed, but is regenerated at the end of the cycle, which proceeds as

$$^{12}\text{C}\ (\text{p},\gamma)\ ^{13}\text{N}\ (\text{e}^{+},\nu)\ ^{13}\text{C}\ (\text{p},\gamma)\ ^{14}\text{N}\ (\text{p},\gamma)\ ^{15}\text{O}\ (\text{e}^{+},\nu)\ ^{15}\text{N}\ (\text{p},\alpha)\ ^{12}\text{C}.$$

The initial Coulomb barrier in the p+^{12}C reaction is higher than in the reactions of the pp chain but, if the temperature is high enough, this chain is faster because it does not involve the very slow p+p fusion reaction (1.3.1). The speed of the CNO cycle is still limited by weak interactions, namely a 10-minute lifetime for the β-decay of ^{13}N, and 2 minutes for ^{15}O. The total energy released in one CNO

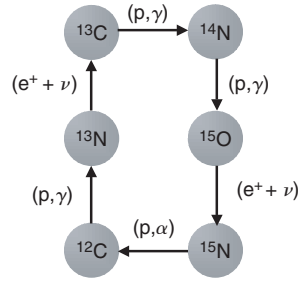

Fig. 1.11. The CNO cycle also converts four protons into one α particle, while the initial ^{12}C is a catalyst that is regenerated at the end of the cycle.

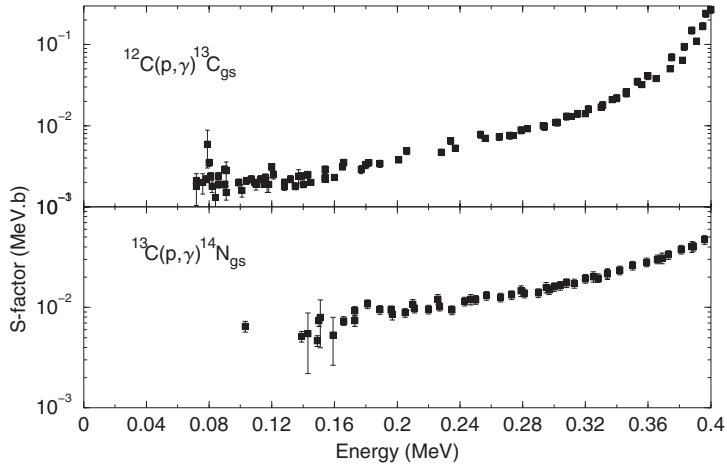

Fig. 1.12. S-factors for the cross sections of two important CNO cycle reactions.

cycle is the same (26.73 MeV) as in the pp chain, if the energy taken by escaping neutrinos is included.

The cross sections (or rather the S-factors) needed in the CNO cycle have to be extrapolated to low energies from those energies where measurements are possible. For the (p,γ) reactions on ^{12}C and ^{13}C, Fig. 1.12 shows that the S-factor extrapolation should be straightforward. For the ^{14}N(p,γ)^{15}O reaction in Fig. 1.13, however, there is a prominent resonance at 278 keV that makes the extrapolation non-trivial. In this case, better results should be expected from a model that is fitted to the resonance and the measured data above the resonance.

The basic CNO cycle returns to its starting point with the proton capture reaction via the production of a ^{16}O compound nucleus in an excited state (represented by ^{16}O*), which subsequently decays to $^{12}\mathrm{C} + \alpha$:

$$^{15}\mathrm{N} + \mathrm{p} \rightarrow {}^{16}\mathrm{O}^* \rightarrow {}^{12}\mathrm{C}_{\mathrm{gs}} + \alpha. \tag{1.3.10}$$

By this reaction, ^{12}C is regenerated at the end of the cycle. Occasionally, however, the excited state ^{16}O* will decay by γ emission. This is when ^{16}O, one of the most important nuclei for later organic life, is finally formed. This ^{16}O may capture another proton, leading to the additional bi-cycle loop shown in Fig. 1.14.

The ^{15}N(p,γ)^{16}O reaction mechanism is influenced even at low astrophysical energies by resonances, especially by the low-energy tail of the 1^- resonance at 338 keV shown in Fig. 1.13. We will see that theoretical models are essential here to determine how the several resonances combine with each other, and also with the non-resonant capture that forms a constant background.

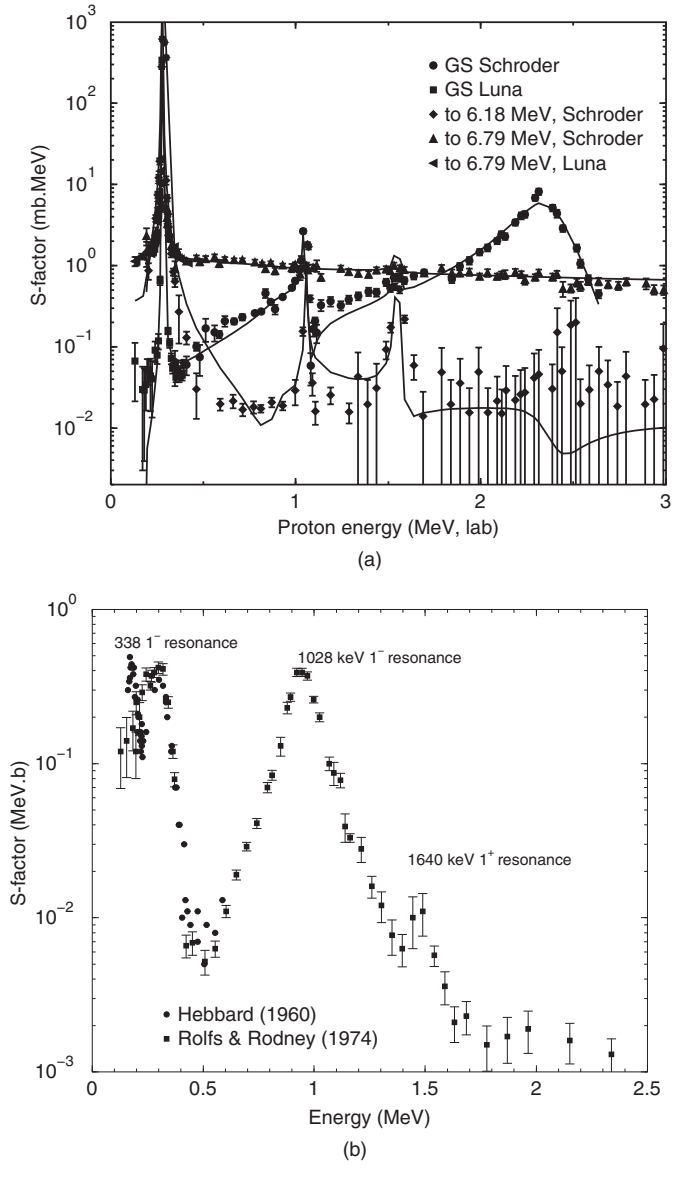

Fig. 1.13. (a) The S-factors for the cross sections of ^{14}N(p,γ)^{15}O reaction, to the ground state, and 6.18 MeV and 6.79 MeV excited states of ^{15}O. The curves are hybrid R-matrix fits discussed in Appendix B. (b) The S-factor for the ^{15}N(p,γ)^{16}O reaction.

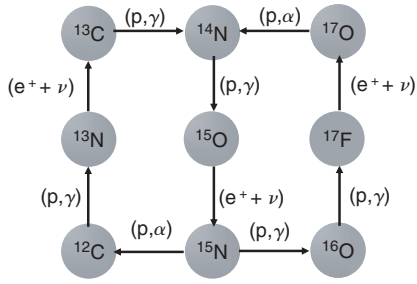

Fig. 1.14. The CNO bi-cycle is a breakout from the original CNO cycle, and produces ^{16,17}O and ^{17}F.

Additional cycles may also occur when a (p,γ) reaction on ^{17}O competes with the (p,α) reaction shown in Fig. 1.14. This leads to a new cycle involving ^{18}F and ^{18}O (not shown here), which after a (p,α) reaction, returns to ^{15}N in Fig. 1.11 and eventually regenerates ^{12}C for continued operation of the CNO cycles.

Eventually no new nuclear reactions are able to produce enough energy to stall further gravitational collapse. In light stars, less than about 8 solar masses, the star gradually contracts into a dwarf star. Outer layers of the star are shed off while the core continues to contract under gravity. If the remaining core mass is less than 1.4 solar masses, then it will compress to electron-degenerate matter, forming a white dwarf.

1.4 Heavy stars

In heavy stars (more than $8\,M_\odot$), all of the above pp, triple-α and CNO cycles occur in early evolutionary stages. These cycles produce residues of carbon and oxygen as before, but now there is sufficient gravitational pressure to compress and heat these residues so that further transmutation reactions may occur: the average thermal energy is sufficient to overcome the Coulomb barriers between the reacting nuclei. In this case, some reaction chains occur which do not eventually cycle back to ^{12}C, initiating the production of heavier elements.

In this section, we will discuss the main processes for heavy element production. In contrast to the production of light elements, here the number of reactions involved is very large and one can no longer enumerate specific reactions. Instead, we will mention the main mechanisms and the astrophysical sites in which these are most likely to occur. Sporadically, we will provide specific examples.

1.4.1 α-burning

Subsequent reactions with α particles, for example, produce heavier nuclei with N and Z both even, namely ^{16}O, ^{20}Ne, ^{24}Mg up to ^{28}Si, which is the dominant residue

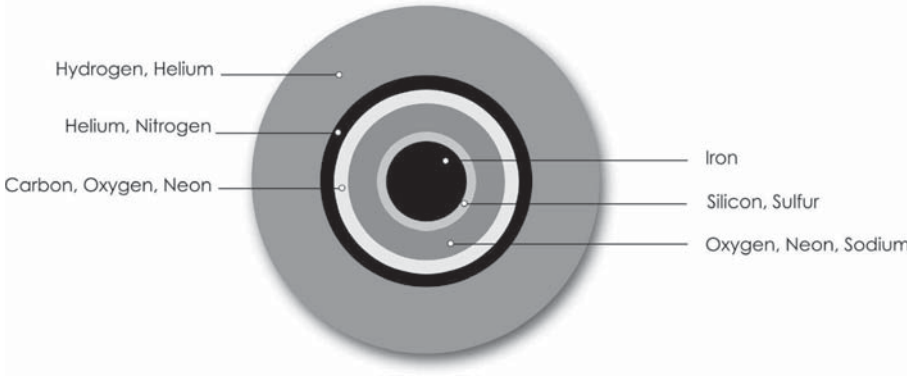

Fig. 1.15. Layers in a red giant star before exploding in a supernova. Figure courtesy of Jon Whiting.

(or 'ash') of the process. These reactions only occur when the temperature is high enough; the Coulomb barriers involved are large because of the increased charge products Z_1Z_2. Some neutrons are also produced by (α,n) reactions, giving rise to nuclei with masses that are not multiples of four.

Stars go through a sequence of carbon, oxygen, neon burning and so on, as the temperature increases with progressively more gravitational contraction. We see from Fig. 1.1, however, that less and less nuclear energy is released in these successive stages, so there is diminishing return of energy in this advanced burning, and the stages pass progressively more quickly. Stars with these reactions, such as red giants in advanced stages of evolution, are therefore less luminous. A diagram of the composition of a red giant is given in Fig. 1.15. Eventually, nuclei near ^{56}Fe are produced (at the core of the massive star), and then no new nuclear reactions are able to produce enough energy to stall further gravitational collapse. This results in a rebound explosion where a new sequence of reactions can occur, to be discussed in Section 1.5.

1.4.2 s-process neutron reactions

Exothermic reactions ($Q > 0$) at temperatures just sufficient to surpass their entrance Coulomb barriers will never produce elements heavier than ^{56}Fe. Even at energies above all the Coulomb barriers, the general decrease of binding seen in Fig. 1.1 for large A implies, via the Saha equation, that the probability of producing, say, ^{208}Pb in equilibrium with ^{56}Fe, is extremely low. However, many heavier elements must be produced somewhere, as we see them in the Sun, according to the measured solar abundances of Fig. 1.16. There must therefore exist sites in

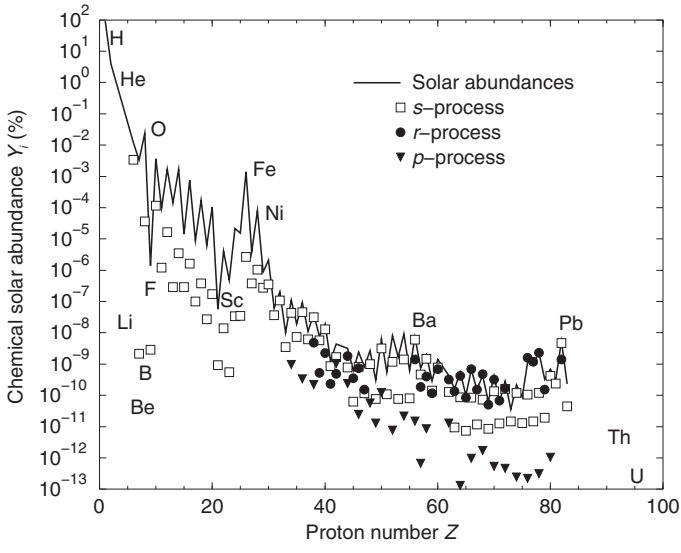

Fig. 1.16. Abundances of chemical elements in the Sun (percentages): observation and the contributions from three important nucleosynthesis processes.

the Cosmos which have sufficiently high temperature to enable the endothermic reactions producing heavy elements, and neutrons should primarily drive the process.

In contrast to proton captures, neutron captures are not hindered at very low energies. We will see later that neutron cross sections rise at low energies as $1/v$ for relative velocity v, and furthermore that the coefficient of v^{-1} *increases* for heavier nuclei. A sequence of neutron capture reactions may thus occur at moderate temperatures generating nuclei as heavy as uranium. This is what is referred to as the *s*-process, the '*s*' for slow.

In red giants (Asymptotic Giant Branch stars) during their α-burning stages, additional neutrons may be produced by (α,n) reactions, for example on ^{13}C or ^{22}Ne. These may be captured by seed nuclei in the iron group, and by progressively heavier nuclei, but at a rate much lower than their β-decay rates. The mechanism for the heavy element production in the *s*-process proceeds with (n,γ) on each stable nucleus (Z, N), producing neutron-rich isotopes $N+1, N+2, \ldots$ This gives nuclei that are a few nucleons away from stability, until a radioactive species β-decays by electron emission to the next element $(Z+1, N_\beta-1)$ in the Segré chart in an isotope with the same mass. This is called a *branching point*. Several branching-point nuclei are identified in Fig. 1.17. New (n,γ) captures can then be repeated on the isotopes with $Z+1$. Through this sequence of (n,γ) and β-decays, most stable

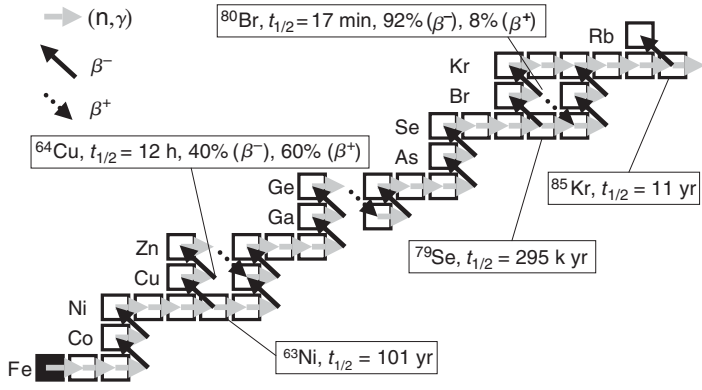

Fig. 1.17. Diagram illustrating the *s*-process with some key branching points.

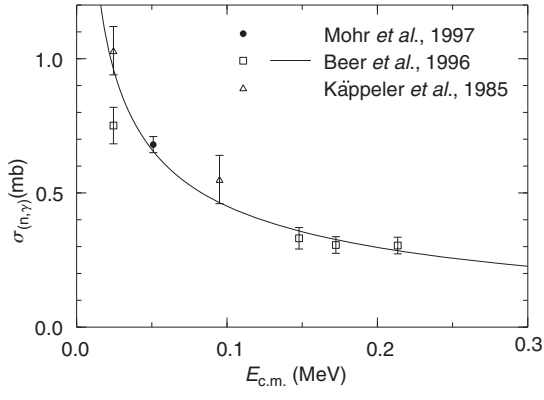

Fig. 1.18. Neutron capture reaction on ^{48}Ca, from [7]. Reprinted with permission from P. Mohr *et al.*, *Phys. Rev C* **56** (1997) 1154. Copyright (1997) by the American Physical Society.

species can be produced, with observable abundance ratios. A diagram illustrating a part of the *s*-process is shown in Fig.1.17. Because the rate of capture reactions is slower than the β-decay rates which bring nuclei back towards stability, the *s*-process proceeds close to the valley of stability in the Segré chart. In Fig. 1.16 we show the contribution of the *s*-process to the solar abundances. Observations of metal-poor stars show that the *s*-process is not universal and depends strongly on the metallicity of the star. This introduces some uncertainties on the final abundances due to the original composition of the star.

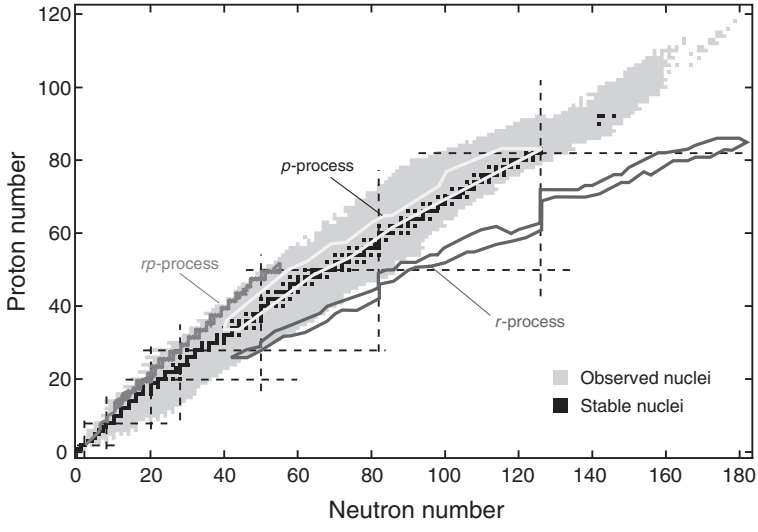

Fig. 1.19. Predicted paths of the *rp*- and *r*-processes, to the left and right, respectively, of the valley of stability. Figure courtesy of Marc Hausmann.

An example of an *s*-process reaction, ^{48}Ca(n,γ)^{49}Ca, has been measured by several researchers [7] and is shown in Fig. 1.18. We will revisit this capture rate when we discuss transfer reactions in Chapter 14 because transfer reactions offer an indirect method for extracting this type of astrophysical information.

1.5 Explosive production mechanisms

The *s*-process alone can only explain about half of the observed abundances of the heavy elements. This has led to a search for astrophysical sites in the Cosmos that are strongly time-varying, and where the equilibrium probabilities are not applicable, enabling an alternate path for the production of heavy elements. The most probable explosive scenario contributing to a large portion of the abundances of heavy elements is core-collapse supernovae. In this environment, high temperatures and a large abundance of neutrons enables a progression of capture reactions extending up to uranium. This is called the *r*-process for *rapid*, as opposed to the *s*-process, which is slow. The capture reactions, however, do not necessarily pass through the stable isotopes, but produce many neutron-rich isotopes that are radioactive, and eventually β-decay into other more stable species well after the explosion has finished. There are also some nuclei that cannot be produced by either the *s*- or the *r*-process mechanisms, suggesting the existence of an additional process which produces the *p*-nuclei. The isotopes involved in the *r*-process and the *p*-process are indicated in the Segré chart, Fig. 1.19.

Although not contributing significantly to the overall production of elements, other explosive environments where the proton density is high give rise to another mechanism, the *rp* (*rapid proton*) process. While the *s*-process proceeds along the valley of stability, the *rp*-process goes along proton-rich paths above and to the left of the valley on the Segré chart, as shown in Fig. 1.19.

1.5.1 r-process neutron reactions

It is widely believed that in supernovae, after core collapse, there are abundant neutrons produced, at least for a few seconds, leading to rapid capture sequences that extend the horizontal isotopic chains to the right, well beyond the first radioactive isotopes (the shaded region in Fig. 1.19). Neutrons are progressively captured by (n,γ) reactions until the production of extremely neutron-rich isotopes is limited by the increased probability of (γ,n) photo-disintegration reactions. This probability increases as the neutrons become less and less bound. The $n \leftrightarrow \gamma$ balance point betweeen capture and disintegration defines the position of the *r*-process path on the Segré chart, and is thought to be between the lines shown in Fig. 1.19. Some of the nuclei that are produced will β-decay to heavier chemical elements (as with the *s*-process), giving a new seed nucleus for another series of neutron captures.

Closed-shell nuclei are usually very stable. These shell closures are believed to be at the places marked by the vertical lines in Fig. 1.19 at $N = 82$, 126, and 184, and here the *r*-process capture times become comparable to β-decay half lives. The rapid process slows down as β-decay wins over neutron capture, and the *r*-process path moves closer to the valley of stability. Nuclei where this happens are known as *waiting points* in the *r*-process. Waiting-point nuclei around $N = 126$ are depicted by the open squares in Fig. 1.20.

The nucleosynthesis produces heavier isotopes until eventually, in the actinide region, fission becomes more probable. It is possible that super-heavy elements ($Z > 114$) may also be produced.

The neutron-rich nuclei will eventually experience a 'freeze-out' after the neutron flux has passed, and will no longer be replenished but will β-decay toward stability. This produces an isotopic population progressively drifting from the neutron-rich side toward the valley of stability. In the Segré chart, this corresponds to a drift diagonally up and to the left from the *r*-process path. In this sense, waiting-point nuclei are the progenitors for the production of stable nuclei of similar mass. The relative abundance of each stable isotope is approximately proportional to the lifetime of its originating nucleus on the *r*-process path. Peaks in the abundance of stable nuclei with $A = 80$, 130, and 192, arise due to the neutron closed shells at $N = 50$, 82, and 126. In Fig. 1.16 we show the contribution of the *r*-process to the solar abundances.

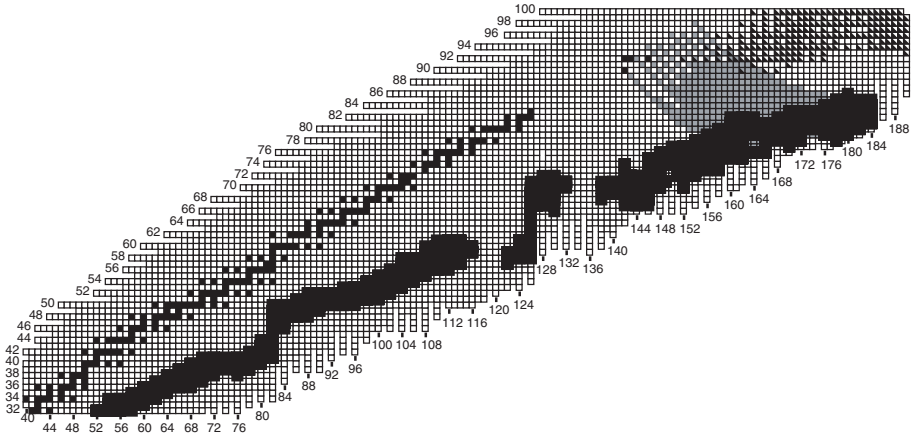

Fig. 1.20. Waiting-point nuclei (black open squares): nuclei produced in the *r*-process and that live long enough to be important signatures in the observed abundances of stable elements [9]. Reprinted with permission from H. Schatz and T. Beers, *Astro. J.* **579** (2002) 625.

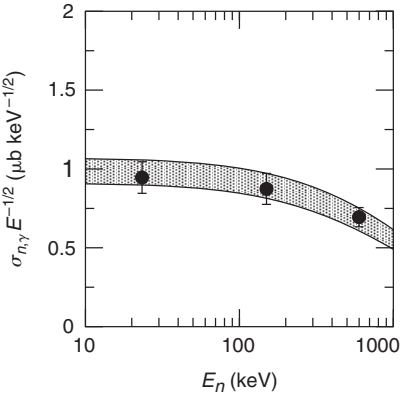

Fig. 1.21. Neutron capture reaction on ^{14}C [8]: comparing direct measurements (black circles) with the (n,γ) extracted from Coulomb dissociation (gray band); for more detail see Chapter 14. Figure courtesy of Neil Summers.

In connection to the *r*-process, we will study later the neutron capture on ^{14}C at very low energies (Appendix B.2.5). This reaction can have strong implications for the final abundances produced in the *r*-process in Type II supernovae. Data for ^{14}C(n,γ)^{15}C direct measurements and cross section determined indirectly from Coulomb dissociation[1] are compared in Fig. 1.21. As seen in Fig. 1.19, most nuclei

[1] A general theory for Coulomb dissociation will be introduced in Chapter 8, and applications discussed in Chapter 14.

involved in the *r*-process have not even been observed. Therefore, at present, the modeling of the *r*-process relies heavily on theory.

Numerous β-decay rates are important inputs to *r*-process network models. There are direct methods to measure this, but alternatively one can determine this information through charge-exchange reactions. In Fig. 1.22, data for ^{58}Ni(t,^{3}He) is shown as a function of the excitation energy of ^{58}Co [10, 11]. The mechanism for these reactions will be introduced in Chapter 4, and a discussion of how to extract the needed structure information from such data will be addressed in Chapter 14. This particular reaction is also very relevant to the mechanism of the explosions in supernovae.

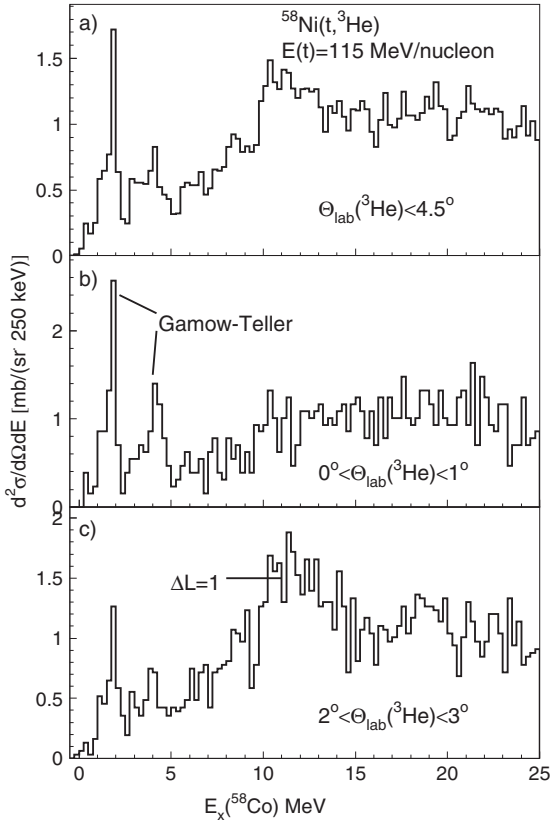

Fig. 1.22. Cross section for the charge exchange reaction ^{58}Ni(t,^{3}He) at 115 MeV/u as a function of the energy of the residual nucleus ^{58}Co [10]. Reprinted with permission from A. L. Cole *et al.*, *Phys. Rev. C* **74** (2006) 034333. Copyright (2006) by the American Physical Society.

1.5.2 The rp-process

The *rp*-process is not required to explain solar abundances but will occur whenever stellar material rich in hydrogen is suddenly heated to high temperatures. Main-sequence stars and red giants will have abundant H and He nuclei evolving according to the normal pp or CNO chains, but in some binary systems, transfers of material from the red giant to the smaller partner will lead to new kinds of thermonuclear explosive reactions.

The preferred sites for the *rp*-process are binary systems involving neutron stars. If there is H-rich massive transfer from the companion to the neutron star, then the temperature and density of that material will suddenly increase as it reaches the surface of the neutron star. There will be a rapid series of (p,γ) and (α,p) reactions that would normally be hindered by the Coulomb barriers, and which will produce a series of proton-rich nuclei up to the $A \sim 60$ mass region. At each step along this *rp*-process, the material may either capture another proton in a (p,γ) reaction, or wait for β-decay. The captures will lead to new isotopes until the proton dripline is reached, or until β-decays become fast enough to compete with the capture processes.

In addition there are intense X-ray fluxes being produced, which have been observed. For this reason, these binary systems are called *X-ray bursters*. With the highest temperatures, nuclei up to $A \sim 100$ may be generated. The *rp*-process becomes progressively hindered by the Coulomb barriers, and remains overall relatively unimportant for the production of nuclei and energy in stars.

A milder version of the *rp*-process can also occur in novae, in accreting material on white dwarfs. However, here, temperatures are not large enough for the process to reach the proton dripline.

1.5.3 The p-process

There are some neutron-deficient isotopes that cannot be made in the *r*- or *s*-processes, which justified naming an additional process. This process is represented by the white line in Fig. 1.19. It involves a sequence of (γ,n), (γ,p), and (γ,α) photo-disintegration on previous-generation stable nuclei. As it is triggered by photons, the process is sometimes called the gamma process.

One of the most likely sites for the *p*-process is in outer layers of core-collapse supernovae, while it heats due to the shock wave passing through it. In the *p*-process, all elements are produced, but in much-reduced quantities when compared to those resulting from the *s*- and the *r*-process. In Fig. 1.16 we show the contributions of the various processes to the abundances in the Sun. It is only for some proton-rich elements that the *p*-process becomes crucial. Also apparent from Fig. 1.19, light nuclei are not fully accounted for by the *s*-process.

1.6 Outlook

1.6.1 Implications for nuclear physics

The nuclides produced in the *s*-process are almost all long-lived enough to be targets in laboratory reaction measurements, and (n,γ) cross sections have been measured for many of these. The *rp*- and *r*-process nuclei, by contrast, have much shorter lifetimes, and are more difficult subjects for laboratory measurements. We will see that some of them have sufficient lifetimes to be produced in radioactive beams, and then used in subsequent secondary reactions to examine their properties. Those with even shorter lifetimes can still be produced as final states in secondary reactions, and some of their properties determined. Reaction theory will be needed to analyze the secondary reactions, and connect those measurements to the reaction rates relevant in astrophysical environments. In the next chapter, we examine nuclear reactions and see what properties of nuclei can be measured, and then in later chapters develop scattering theory so that we have a theoretical framework to describe these nuclear reactions. Eventually, in later chapters, we will close the circle by applying the various reaction theories to many of the astrophysical reactions we introduced in this chapter.

1.6.2 Nuclear astrophysics: an open field

Although the rest of the book focuses on the description of nuclear reactions, these contribute in multiple ways to many open questions in astrophysics. In all the standard processes producing the elements described in this chapter, there are abundance mismatches that need better constraints from nuclear physics, in particular, nuclear structure and nuclear reaction input. One of the greatest challenges has been blending nuclear physics input with astrophysics modeling in a way that meaningful constraints on the parameters can be made. In present-day modeling, there are specific conditions that need to be introduced artificially and are yet awaiting a better understanding. In some cases, there is uncertainty on the nucleosynthesis path (as in the *r*-process); in others, there is uncertainty on the endpoint (as in the weak *s*-process). Perhaps even more exciting are the new emerging ideas that have not been discussed here. There is the weak *s*-process introduced earlier to account for the light nuclei, but more recently the Light Element Primary Process (LEPP) was added to the list, to explain the early galactic adundances and, maybe related to it, the neutrino *p*-process, thought to occur in all core-collapse supernovae, and a possible site for the production of Sr and other elements beyond Fe in very early stages of galactic evolution. Studies aiming for a better understanding of the Universe will continue for decades to come. For more detailed information on astrophysics and the topics covered in this chapter we refer

to textbooks such as Clayton [12], Rolfs and Rodney [13], Arnett [14], Pagel [15], Iliadis [16] and Bennett [17].

References

[1] L. Kawano, Fermi National Accelerator Laboratory, Report FERMILAB-Pub-92/04-A (1992).
[2] P. D. Serpico, S. Esposito, F. Iocco, G. Mangano, G. Miele and O. Pisanti, *J. of Cosm. and Astro. Phys.* **12** (2004) 010.
[3] R. G. H. Robertson, *Prog. Part. Nucl. Phys.* **57** (2006) 90.
[4] F. Hoyle, *Astro. J. Suppl.*, **1** (1954) 121.
[5] H. O. U. Fynbo *et al.*, *Nature*, **433** (2005) 136.
[6] T. A. Weaver and S. E. Woosley, *Phys. Rep.* **227** (1993) 65.
[7] P. Mohr *et al.*, *Phys. Rev. C* **56** (1997) 1154.
[8] N. C. Summers and F. M. Nunes, *Phys. Rev. C* **78** (2008) 011601R; *Phys. Rev. C* **78** (2008) 069908.
[9] H. Schatz and T. Beers, *Astro. J.* **579** (2002) 626.
[10] A. L. Cole *et al.*, *Phys. Rev. C* **74** (2006) 034333.
[11] R. Zegers, NSCL White Paper 2007.
[12] D. D. Clayton 1984, *Principles of Stellar Evolution and Nucleosynthesis*, Chicago: University of Chicago.
[13] C. E. Rolfs and W. S. Rodney 1988, *Cauldrons in the Cosmos*, Chicago: University of Chicago.
[14] D. Arnett 1996, *Supernovae and Nucleosynthesis*, Princeton: Princeton University Press.
[15] B. E. J. Pagel 1997, *Nucleosynthesis and Chemical Evolution of Galaxies*, Cambridge: Cambridge University Press.
[16] C. Iliadis 2007, *Nuclear Physics of Stars*, Weinheim: Wiley.
[17] J. Bennett, M. Donahue, N. Schneider, M. Voit, *The Essential Cosmic Perspective*, San Francisco; Toronto: Addison-Wesley.